

Low-power magnetized microdischarge ion source

Cite as: Appl. Phys. Lett. **89**, 061501 (2006); <https://doi.org/10.1063/1.2335612>

Submitted: 08 December 2005 . Accepted: 02 July 2006 . Published Online: 08 August 2006

Tsuyohito Ito, and Mark A. Cappelli



View Online



Export Citation

ARTICLES YOU MAY BE INTERESTED IN

[Self-organization in planar magnetron microdischarge plasmas](#)

Applied Physics Letters **106**, 254104 (2015); <https://doi.org/10.1063/1.4922898>

[Electrostatic probe disruption of drift waves in magnetized microdischarges](#)

Applied Physics Letters **94**, 211501 (2009); <https://doi.org/10.1063/1.3132587>

[Comparison of hybrid Hall thruster model to experimental measurements](#)

Physics of Plasmas **13**, 083505 (2006); <https://doi.org/10.1063/1.2336186>



Your Qubits. Measured.

Meet the next generation of quantum analyzers

- Readout for up to 64 qubits
- Operation at up to 8.5 GHz, mixer-calibration-free
- Signal optimization with minimal latency

Find out more



Low-power magnetized microdischarge ion source

Tsuyohito Ito^{a)} and Mark A. Cappelli

Mechanical Engineering Department, Stanford University, Stanford, California 94305-3032

(Received 8 December 2005; accepted 2 July 2006; published online 8 August 2006)

The authors report on the design and operation of a magnetized microdischarge ion source. The discharge is a coaxial ($\mathbf{E} \times \mathbf{B}$) configuration with a closed-electron drift. Conditions are selected such that the ions are nonmagnetized and the electrons strongly magnetized. The operating characteristics of this ion source are studied in the 10–40 W power range, generating a total ion current as high as 0.15 A and a peak ion energy of ~ 150 eV at an operating voltage of 200 V. The ionization efficiency approaches 100%, although the present design has a fairly large ion beam divergence ($\sim 80^\circ$ half-angle). The compact nature of this ion source is suitable for localized processing or can be easily clustered for multi-ion processing. © 2006 American Institute of Physics. [DOI: 10.1063/1.2335612]

There is a growing interest in the development of microplasmas, micro-discharges, or microion sources for a range of applications. For example, the most widely recognized application is the use of individually addressed dielectric barrier microdischarges in plasma displays. However, they have also been used in local etch processing,¹ chemical analysis,² and surface treatment/modification,³ amongst other applications. A common feature of microdischarges is that they can be ignited and sustained at relatively high pressure, removing the need, in some cases, for vacuum chambers. High pressure operation is a natural consequence of the pressure-discharge (p - d) gap scaling. However, a trade-off of this is the operation in a highly collisional environment, which precludes applications that may require high ion energy. The generation and operation of a microdischarge at very low pressures and low powers may open fields of applications that benefit from concentrated, high current density, and highly energetic ions, such as in spatially constrained surface treatment or modification, sputtering, and low energy ion implantation.

In this letter, we report on the design and operation of a low-power magnetized microdischarge ion source. Conditions are selected so that the electrons are highly magnetized, but the ions are not. This leads to the generation of a high current density, high energy ion stream at relatively low background pressure. The design of this microdischarge is motivated by higher power versions, commonly referred to as closed-electron drift Hall accelerators, used in space propulsion applications. A scaled down version of an anode-layer Hall accelerator operating at the 50 W level has been previously presented.⁴ The discharge developed here has a higher magnetic field strength and a configuration that better resembles the so-called stationary plasma thruster. In the studies of Ref. 4, significant overheating of the discharge precluded operation for extended time at optimal conditions. This is an expected consequence of the scaling of Hall discharges to smaller sizes.^{4,5} In the discharge presented here, the high heat load is accommodated by the use of thick film diamond for thermal management and by water cooling the iron base.

A schematic of the cross section and photograph of the ion source are shown in Fig. 1. The magnetic field is used to

establish the resistive electric field which confines and heats the electrons. The magnetic circuit incorporates a ring-shaped SmCo permanent magnet together with a high purity iron core to form the poles. The outer diameter of the magnet is 14 mm, the inner diameter is 4 mm, and the thickness is 3 mm. The outer diameter of the iron core is 3 mm, resulting in an annular channel of width $w=0.5$ mm. The insulator outer wall depth, which is the thickness of the alumina insulator covering the magnet, is $230 \mu\text{m}$. The magnetic field

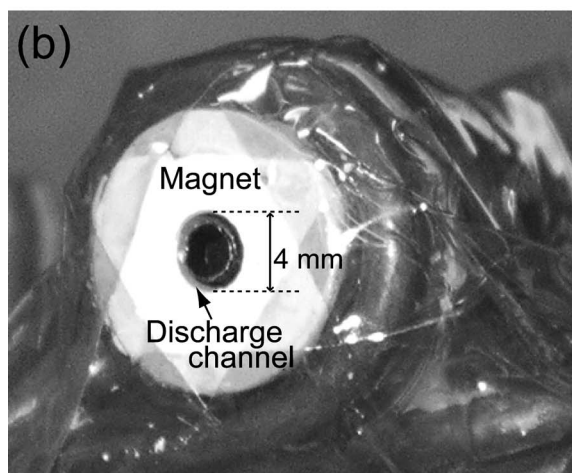
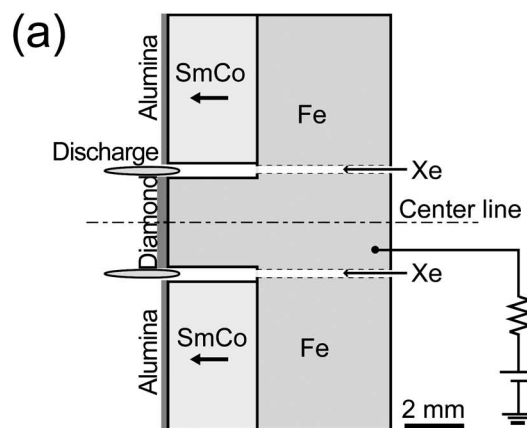


FIG. 1. (a) Schematic cross section and (b) photograph of the magnetized microdischarge ion source.

^{a)}Electronic mail: tsuyohito@stanford.edu

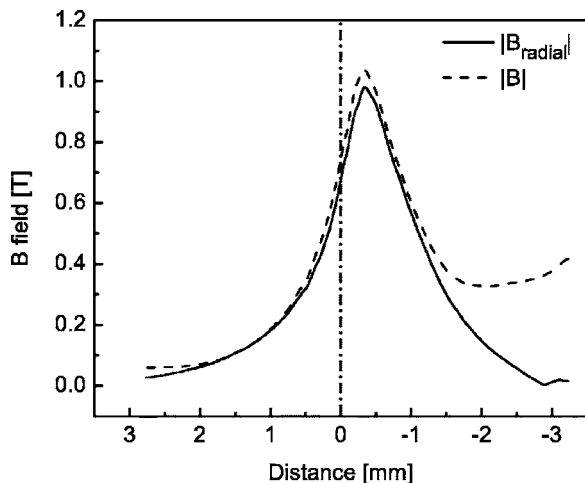


FIG. 2. Computed magnetic field strength and radial component of the magnetic field, along the center of discharge channel. The position of 0 mm corresponds to the exit of the channel. Negative positions correspond to the region upstream of the exit (inside the channel).

generated by this structure is predominately radial near the exit of the channel, as verified by simulations for this circuit carried out using a finite element solver.⁶ Figure 2 shows the simulated magnetic field (radial component and the magnitude) along the center of the channel where a position of 0 mm corresponds to the channel exit (the surface of the alumina insulator). The magnetic field strength near the exit of the channel is ~ 0.7 T. At this field strength, the electron Larmor radius $L_e \sim 15 \mu\text{m}$ (using electron temperature T_e of 10 eV), and electrons should be strongly magnetized, since $L_e \ll w, \lambda_e$. Here, λ_e is the electron mean free path, estimated to be at most ~ 1 cm (assuming the pressure higher than 10^{-3} Torr), near the exit of the channel. Ions created in this electron confinement region are unaffected by the magnetic field because of their large mass, and are rapidly accelerated out of the channel by the electric field to nearly collisionless conditions, as the background chamber pressure is very low ($\sim 10^{-5}$ Torr), as discussed below.

For the studied described here, xenon (Xe) is used as a source gas, injected into the channel at its base through eight small holes, 0.33 mm in diameter. The flow rate was controlled by a 0–5 SCCM (SCCM denotes cubic centimeter per minute at STP) mass flow controller. The iron core serves

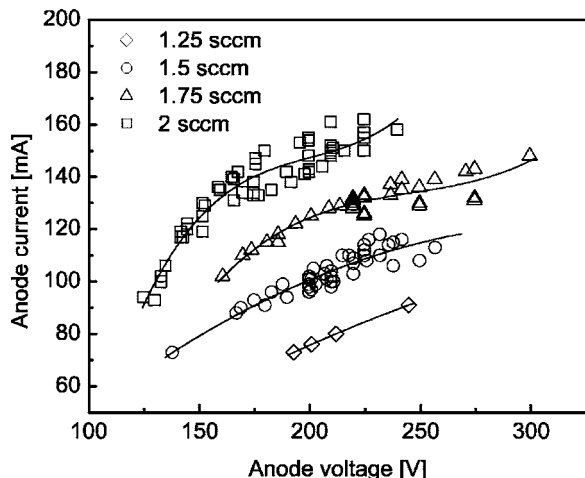


FIG. 3. I - V characteristics in voltage-limited operation.

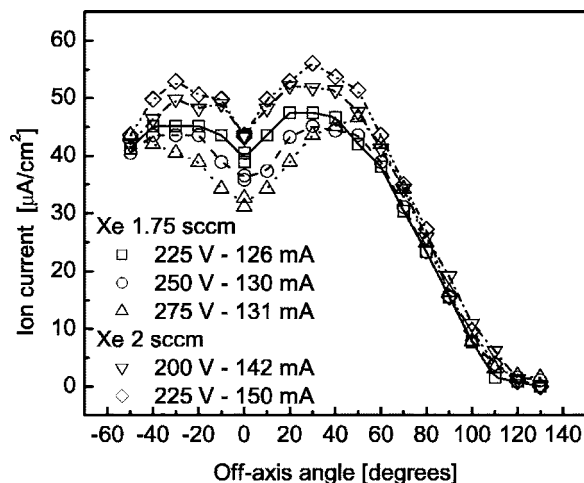


FIG. 4. Angular sweeps of the ion current density distribution in the beam, 22 cm downstream of the discharge exit.

as the anode of the discharge, and is connected to a laboratory power supply operated in voltage-controlled mode. For thermal management, the iron base is water cooled, and the central pole piece is covered with a 3 mm diameter, 400 μm thick polycrystalline diamond plate. All data reported in this letter were taken with an external hollow cathode (Ion Tech, Inc., HCN-252) operating with a flow of 1.6 SCCM of xenon. The cathode was positioned 1 cm downstream and 4 cm off axis of the discharge. It is noted that similar results are obtained with a thoriated tungsten filament cathode. The ion source was operated in a nonmagnetic stainless steel chamber approximately 0.6 m in diameter and 1.2 m in length, serviced by a single 55 cm diameter cryopump (CVI-TM500), capable of a base pressure of approximately 10^{-6} Torr. The background chamber pressure settles to $\sim 10^{-5}$ Torr with 2 SCCM of Xe flow through the anode. It is noteworthy that the local discharge pressure in the ionization region near the channel exit can be much higher ($\sim 10^{-3}$ – 10^{-2} Torr).

During operation, the discharge generated intense blue emission (due to xenon ions) in the annular channel. Representative current-voltage (I - V) characteristics are shown in Fig. 3. The current tends to “saturate,” with increased voltage, possibly due to having achieved a high degree of ionization. A guarded planar ion probe (3 mm in diameter) biased to ~ -30 V to repel electrons drawn from the cathode to neutralize the beam was used to measure the ion current distribution and total ion current in the beam. The ion current measurements were performed 22 cm downstream of the channel exit. The ion energy distribution was characterized by a miniaturized retarding potential analyzer (RPA), with a 4 mm entrance aperture. For the RPA measurements, the outermost grid is electrically floating, the second (electron repelling) grid was set to a potential of -25 V, and the ion retarding grid was swept to a potential of $\sim +350$ V. The collector was coated with graphite emulsion, to reduce secondary electron emission. The transmitted ion-current incident onto the collector was recorded with a picoammeter. For the ion energy measurements reported here, the entrance of the RPA was located 7 cm downstream of the channel exit. Both the ion probe and RPA were mounted on a stepper motor-controlled rotational stage for angle-resolved measurements.

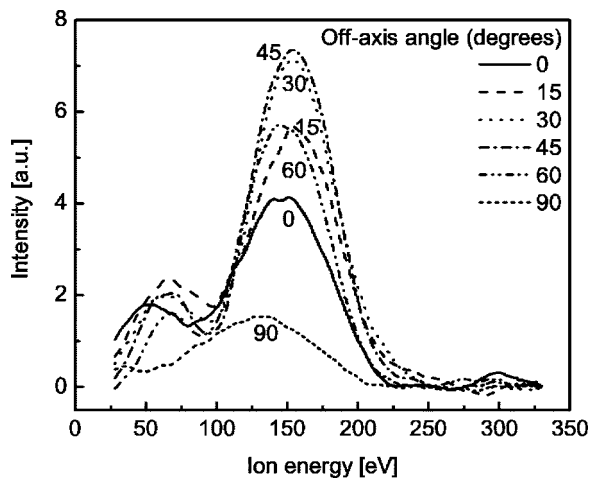


FIG. 5. Angle-resolved ion energy distribution for conditions corresponding to a Xe flow rate of 2 SCCM, 200 V anode potential, and 148 mA total discharge current.

The angular distribution in the beam ion current distribution is shown in Fig. 4. It is apparent that for this initial discharge design, the beam diverges considerably, with a e^{-1} half-angle of $\sim 80^\circ$. There is a noticeable depression in current along the axis, with the current density peaking at an angle of $\sim 30^\circ$. The current density distribution is relatively symmetric, and by integration over the extrapolated distribution for the half-space, we obtain an estimated total ion current of ~ 130 mA for the 200 V, 2 SCCM operating condition. It is noteworthy that the total discharge current for this condition was measured to be ~ 142 mA, indicating that the fraction of the total electron current from the cathode used to service the discharge is $\sim 10\%$ (the balance of which is carried along with the ion beam, for beam neutralization). Another measure of ion source performance is the ionization efficiency, defined here as the total ion current, divided by the ion current expected if all of the xenon is singly ionized. The ionization efficiencies are estimated to be 85%–95% for conditions of 2 SCCM and a voltage of 175–225 V, and 90%–100% for 1.75 SCCM and a voltage of 225–275 V. Considering the error estimated from the reproducibility in the total ion current ($\sim 20\%$) and the possibility of some small fraction of doubly ionized xenon in the beam, these measurements confirm that this discharge source has a high ionization efficiency.

The angle-resolved ion energy distribution for a discharge voltage of 200 V and xenon flow of 2 SCCM is shown in Fig. 5. It is noted here that these distributions represent that of ions that may impinge onto a grounded surface. The distribution is dominated by energetic ions peaked at a potential of ~ 150 eV, approximately 50 eV lower than the discharge voltage. This 50 eV energy deficit seemed to be independent of the operating conditions. Most scans exhibit a low energy peak in the range of 50–60 eV. We believe that

this peak may be due (mostly) to backward-scattering collisions between the ions in the beam and neutral xenon emitted by the hollow cathode, because this peak was not as apparent when the discharge was operated with a filament cathode. However, this low-energy peak may also reflect the presence of backward-scattering collisions with nonionized xenon exiting the anode, because it was not as strong for operating conditions at the lower anode flow rates.

For many applications, the relatively high beam divergence observed in this initial design is undesirable. We believe that the high beam divergence is a result of the qualitative observation that the ionization zone seems to be somewhat downstream of the channel exit, where there is a strong divergence in the magnetic field. We attribute this misplacement of the ionization zone to the short circuiting of the electron confinement by electron collisions with the front face and channel wall near the end of the channel, where the magnetic field is strong. A future design will widen the channel, and modify the field to generate a partial mirroring effect that will reduce direct electron-wall scattering. This is expected to move the ionization zone into the channel where the equipotential contours are more orthogonal to the channel walls, resulting in a concomitant reduction in beam divergence.

The ion source described here generates ions at a cost (defined as the amount of discharge power required to produce 1 A of ion current) of approximately 200 eV/ion. This is about a factor of 2–3 larger than some macroscale discharges, such as helicon discharges. However, this is not unexpected, as these other discharges operate at much larger volume to surface area ratios, and consequently much lower overall surface energy flux. The compact and relatively simple design, along with the high current (~ 0.15 A), makes this a potentially useful ion source in space-constrained applications. Multiple sources in close proximity can be easily arranged to provide independently controlled exposure to different ion species.

This research was supported in part by the NSF/DOE Basic Plasma Initiative, and by the Air Force Office of Scientific Research. The authors would like to thank W. S. Crawford, N. Gascon, and M. Bachand for their technical assistance and helpful discussions. Partial support for one of the authors (T.I.) was provided by JSPS.

¹R. M. Sankaran and K. P. Giapis, *Appl. Phys. Lett.* **79**, 593 (2001).

²C. Brede, S. Pedersen-Bjergaard, E. Lundanes, and T. Greibrokk, *Anal. Chem.* **70**, 513 (1998).

³H. Yoshiki, A. Oki, H. Ogawa, and Y. Horiike, *J. Vac. Sci. Technol. A* **20**, 24 (2002).

⁴V. Khayms and M. Martinez-Sanchez, 32nd Joint Propulsion Conference, Lake Buena Vista, FL, 1996, Paper No. AIAA-1996-3291.

⁵D. P. Schmidt, N. B. Meezan, W. A. Hargus, Jr., and M. A. Cappelli, *Plasma Sources Sci. Technol.* **9**, 68 (2000).

⁶D. C. Meeker, *Finite Element Method Magnetics*, Version 3.4.1, <http://femm.foster-miller.net>